INTERNATIONAL JOURNAL OF
COASTAL, OFFSHORE & ENVIRONMENTAL ENGINEERING IJCOE Vol.9/No.3/Summer 2024/ (43-57)

Available online at: www. Ijcoe.org

Ecological modeling of pollutant removal in urban wetlands

Parand Bamdadi[1], Ozeair Abessi[11], Hassan Amini Rad[1]

[1] *School of Civil Engineering, Babol Noshirvani University of Technology, Babol, Iran*

ARTICLE INFO

Article History:
Received: 22 June 2024
Accepted: 7 Sep. 2024

Keywords:
Wetland
Numerical Modeling
Purification
Hydrodynamic

ABSTRACT

Wetlands are unique, diverse, and productive habitats in the natural environment. They have significant ecologic values due to their potential to deposit, sediment, and filter out pollutants from the water that flows through them. Wetlands have been investigated from different aspects in the past years; however, the computer modeling of the complex processes that occur in wetlands has attracted less attention. In this study, the mechanism of pollutant removal has been studied by developing a new template for the ecological modeling of the wetlands. The kinetics of oxygen balances, biochemical oxygen demand, coliform, and nutrient removal are numerically simulated. To explore modeling capabilities, a wetland in northern Iran, was investigated as a case study. Field measurements were performed for parameter estimations and model calibration. The numerical results exhibited that concentrations of BOD, total coliform, phosphate, and nitrate decreased up to 45%, 44.96%, 44.8%, and 43.47%, in the outflow when model has run for spring and summer seasons and the results compared to the field sampling data.

[1] Corresponding Author. Babol Noshirvani University of Technology, Shariati Ave., Babol, Mazandaran, Iran, P.O. box: 484, Postal Code: 47148 – 7116, Tel: +98 (11) 3550 1075, E-mail address: Oabessi@nit.ac.ir

1. Introduction

Today, urbanization is increasing, all around the world. About four billion people, half of the world's population, now live in urban areas and this ratio will reach 66% by 2050 due to the migration of people to cities hoping to find jobs and a more active social life [1]. Cities make up 80% of the world's economic values and contribute fundamentally to world purposes for sustainable development goals [2]. Meanwhile, urban sprawl has raised concerns as a significant threat to natural resources by destroying the cities' marginal lands, i.e., forests, farms, and wetlands. The loss of wetlands, which are among the first casualties of such a blind and unsustainable development system, has been reported to constantly destroy wildlife habitats and biodiversity mostly around the urban areas [3]. In return, experts believe that if the wetlands were left untouched and protected, they would make cities more habitable and environmentally compatible [4-6].

Wetlands used to be considered worthless lands and were used as landfills or places for wastewater disposal in some parts of human history. Recently and after the Ramsar convention (1971), wetlands' aesthetic and other benefits for recreation, agricultural purposes, conservation, and water quality improvements have been highlighted [3]. Ramsar Convention draws significant attention to the wetlands' environmental functions and their socio-economic benefits for human societies [7]. Today, however, wetlands are globally valued and cherished for their role in improving water quality, flood attenuation, biodiversity, supporting aquatic habitats, and cultural, social, and economic services [3, 8].

Wetlands are pollution-catching powerhouses and can trap nitrogen and phosphorous with a unique potential. Wetlands can enhance compounds' retention by storing sediment, nutrients, and heavy metals and facilitate treatment by digesting organic compounds due to aerobic and anaerobic processes [8]. The ability of the wetlands to purify contaminations makes them an ideal treatment area for anthropogenic and natural pollutants. Such diverse capabilities made a growing interest in the simultaneous use of wetlands as a source of water, a place for pollution removal, and a recreation center for those wetlands located inside or near urban areas.

In the last few years, many investigations have been reported on the wetlands' efficiency for contamination removal [9-13]. Hammer [9] provides a detailed analysis of wetlands pollutant removal capabilities by reviewing the case studies from constructed wetland projects worldwide [9]. Craft et al. [10] overviewing the findings from numerous studies, focused on the removal processes of nitrogen, phosphorus, and sediment by the wetlands. The article discussed the importance of wetland design, vegetation, and hydrological conditions in achieving optimal removal rates. Mitsch and Gosselink [11] provide a holistic overview of wetlands ecology and their role in pollution removal through covering removal mechanisms on nutrients, heavy metals, and organic contaminants. Vymazal and Kröpfelová [12] reported an in-depth analysis of nutrient removal in different types of constructed wetlands. To optimize nutrient removal, they provide deep insights into the design and management practices of the constructed wetlands. Vymazal [13] discussed the role of plants, microorganisms, and substrates in enhancing pollutant removal in wetlands. Vymazal provided case studies and performance data from various constructed wetland systems.

Besides numerous field and laboratory studies, there has been always an ambition to develop a sort of interactive mathematical model to simulate wetland's ecological processes with the computer. Only recently and after new advancements in computing power and simulation techniques it has become possible. Through integrating hydrodynamics, water quality, and ecological processes, computer models are becoming able to provide a comprehensive understanding of wetlands' function as a pollution control measure.

So far, a few computer modeling techniques have been reported for the interactive simulation of wetlands' processes [14-20]. Somes et al. [14] used MIKE21 for the simulation of flow hydrodynamics in the Monash University Research wetland. Field data for six months were used for the model calibration, and the results show good agreement between the numerical model and field observations. Kazezyilmaz-Alhan et al. [15] developed a comprehensive hydrological and water quality model (Wetland's Solute Transport Dynamic, WETSAND) for surface flow and solute transport in a constructed wetland. The model incorporates surface water/groundwater interactions and accounts for upstream contributions from urbanized areas. Boutilier et al. [16] studied the fate and transport of E. coli bacteria in a full-scale surface flow wetland for treating domestic wastewater using the WASP model. The model was able to predict the average concentration of E. coli successfully but was not accurate in predicting the maximum and minimum number of E. coli in the wetland. Hydrodynamic and ecological laboratory (ECO Lab) modules of MIKE21 were used by Suntoyo et al. [17] to evaluate the water quality of the Porong River in the Madura Strait, Indonesia. The dispersion and dynamic of COD, TSS, phosphate, and nitrate were calculated and compared with the standard after model calibration with the field data at 4 different locations. Qiao et al. [18] also used MIKE21 to simulate the hydrodynamic properties and salinity transport in the Pink Beach wetland of the Liao River estuary, China. The effects of wetland plants on tidal flows were also investigated by

changing the Manning coefficient. Internal hydraulics and the effect of wind on the surface flow in a constructed wetland that is fed via agricultural drainages were investigated by Pugliese et al. [19]. The results showed that shallow areas with the wind in the opposite direction of the flow would lead to more mixing and rotation in the wetland. Thu Minh et al. [20] used MIKE 11 to quantify the spatiotemporal dynamics of water quality parameters in the Long Xuyen Quadrangle area of the Vietnamese Mekong Delta.

Reviewing the literature showed that developed computer models up to the current time were less interactive and limited to considering removal processes in the wetlands. The aeration processes and the dynamics of oxygen balance (O2 aeration and consumption) were not simulated and the influx of the hydrodynamic model on the ecological process was not fully considered. So, the current study aimed to provide a new template for the comprehensive ecological simulation of urban wetlands with a high inflow of domestic sewage. To reach the goal, the influencing processes on organic pollutant removal were extracted and a detailed insight into the transport, transformation, and degradation processes for each was provided. So a three-dimensional numerical model has been developed using MIKE 3 Flow Model (FM) and ECO Lab Module. ECO Lab interconnects hydrodynamic, water quality, and ecological processes and provides a possibility to modify or create the formulation that is needed for a specific water body. As a case study, the customized model has been tested for the Gole-Niloufar wetland, located in north of Iran. In the model, the processes of DO, BOD and coliform degradation, together with Nitrate and Phosphate removals were formulated through the causal relations that describe each specific phenomenon. For calibration purposes, a series of field measurements in even days of one month, and for model validation, sampling in different seasons of one year was performed and the results were tested and verified against the field data.

2. Materials and methods

The Flow Model (FM) along with ecological laboratory (ECO Lab) modules of DHI MIKE3 software are used to simulate the hydrodynamic and ecological features of the wetland. In the enclosed water bodies where species stratification occurs, the three-dimensional model should be used [21, 22]. The virtue of this modeling technique is that the hydrodynamic model is simultaneously interacting with the results of the ecological model. As a result, pollutants' mixing and dispersion and their decay and deposition due to aeration, evaporation, sunlight, bacterial decomposition, and plant uptake processes can be modeled at a time, more interactively. The modeling framework of this study is depicted in Figure 1.

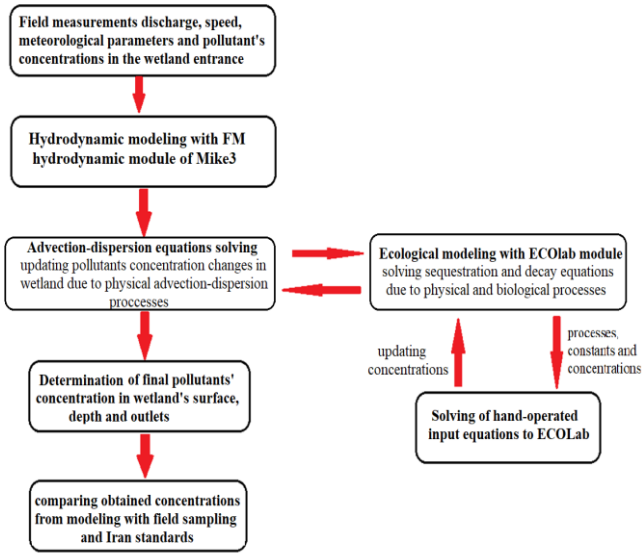

Figure 1. The overview of the modeling framework

2.1. Hydrodynamic model

The hydrodynamic or Flow Model (FM) is a standard MIKE3 tool for flow simulation in water bodies with three-dimensional structures, such as wetlands, bays and coastal areas. This model can simulate unsteady flows with density changes and external forces, including meteorological and tidal parameters [21]. The model is based on a flexible mesh method. The z-direction discretization can be either a sigma coordinate or a sigma/z-level coordinate, which uses a cell-centered finite volume method. The elements of unstructured mesh in x-y coordinate can be generated as triangular or quadrangular elements [22].

Mathematical modeling in the MIKE3 is based on the Navier-Stokes equations. It solves mass and momentum conservation equations and salinity and temperature transport equations with the help of the Reynolds-averaged method in three dimensions. In the Reynolds-averaged method, all the turbulent fluctuations are modeled and represented in terms of the mean-flow characteristics [23-24]. Therefore, the computational expenses for simulation are dramatically reduced, and solving the governing equations becomes possible for real engineering applications. These equations can be written in the Cartesian coordinate as follows [25]:

$$\frac{1}{\rho C_S{}^2}\frac{\partial P}{\partial t}+\frac{\partial u_j}{\partial x_j}=SS \qquad (1)$$

$$\frac{\partial u_i}{\partial t} + \frac{\partial (u_i u_j)}{\partial x_j} + 2\Omega_{ij} = \frac{1}{\rho}\frac{\partial P}{\partial x_i} + g_i + \frac{\partial}{\partial x_j}\left(v_T\left(\frac{\partial u_i}{\partial x_i} + \frac{\partial u_j}{\partial x_j}\right) - \frac{2}{3}\delta_{ij}\right) + u_i SS \quad (2)$$

$$\frac{\partial C}{\partial t} + \frac{\partial}{\partial x_j}(Cu_j) = \frac{\partial}{\partial x_j}\left(D_s \frac{\partial C}{\partial x_j}\right) + SS \quad (3)$$

$$\frac{\partial T}{\partial t} + \frac{\partial}{\partial x_j}(Tu_j) = \frac{\partial}{\partial x_j}\left(D_T \frac{\partial T}{\partial x_j}\right) + SS \quad (4)$$

Where t is the time, ρ is the density of the water, C_s is the speed of sound in seawater, u_i is the velocity in the x-direction, Ω_{ij} is the Coriolis force tensor, P is the fluid pressure, g is the gravitational acceleration, ν_T is the turbulent eddy viscosity, δ is Kronecker's delta, k is the turbulent kinetic energy, S and T are salinity and temperature, D_S and D_T are linked to dispersion coefficients. SS states as the respective source-sink terms, which is different from the equation to the equation.

In the flow model of Mike3, bed resistance can be identified as no bed resistance, quadric drag coefficient, and roughness height. In this study, a constant roughness height is considered. The bottom stress is calculated from the equation below:

$$\frac{\overline{\tau}_b}{\rho_0} = c_f \overline{u}_b |\overline{u}_b| \quad (5)$$

Where $\overline{u}_b$ is the flow velocity at Δz_b above the bottom, ρ_0 is the water density, c_f is the drag coefficient and is determined by the (6) equation:

$$c_f = \frac{1}{(\frac{1}{k}\ln(\frac{\Delta_{z_b}}{z_0}))^2} \quad (6)$$

In this equation, k is the von Kármán constant considered 0.4 and z_0 is the scale of bed roughness length. Generally, the roughness height range is between 0.01-0.3 m. The roughness value directly relates to friction, as considered in the model [25].

2.2. Ecological model

This study tried to consider major physical, chemical, and biological processes in the wetland. Therefore, a new template in the ecological laboratory module of MIKE has been developed to simulate pollution removal processes considering climate factors such as temperature, wind, natural aeration, evaporation, and sunlight together with the natural procedures of sedimentation, degradation, and bacterial and plant uptakes. ECO Lab is a flexible numerical laboratory for the ecological modeling of natural ecosystems. So as a process equation solver, it can calculate the rate of change of state variables, processes, and forces. The MIKE ECO Lab provides an open space for manual input of the equations for the reaction rate of state variables. One can make more accurate predictions with built-in templates or create a new model concept containing the necessary causal relations to describe a specific problem. The model can simulate the processes of transfer, dispersion, and degradation of pollution, in the simultaneous operation of the hydrodynamic model. Processes express the rate at which variables change in the wetland environment [25]. This change can be expressed as a set of coupled ordinary equations:

$$P_c = \frac{dc}{dt} = \sum_{i=1}^{n} process_i \quad (7)$$

In this equation, c is the state variable concentration in the module, and n is the number of processes involved for a particular state variable [25]. The processes are:

2.2.1. Oxygen balances

Modeling of the oxygen balance depends on the level of complexity chosen. There are four levels of complexity to describe the mass equation for DO. In this study, level 3 of the oxygen balance equations has been used, in which, besides the oxygen, changes in the concentration of nutrients are also effective:

$$\frac{dDO}{dt} = +reaeration - \text{BODdecay} - Y_1.nitrification + photosynthesis - respiration - sediment\ oxygen\ demand \quad (8)$$

Equation (8) includes aeration, nitrification, BOD degradation, photosynthesis, respiration, and the amount of oxygen demanded by sediments. Y1 is the yield factor for oxygen [25-26]. According to previous studies, Y1 ranges between 1.2 and 1.8, depending on the value of F/M (food/microorganism [27].

- **Aeration**

This is a process that describes the exchange of oxygen between dissolved oxygen and the atmosphere. This term refers to the level of oxygen saturation in water Cs, which depends on salinity and temperature.

$$d(\text{reaeration})/_{dt} = K_2(C_s - DO) \quad (9)$$

K_2 is the rate of the aeration process, which depends on W_V wind speed, V velocity, and water depth H, and its unit is 1/s:

$$K_2 = \frac{3.93V^{0.5}}{H^{1.5}} + W_V/H \quad (10)$$

W is obtained from the following equation, and its unit is m/s.

$$W_V = 0.728{W_V}^{0.5} - 0.371W_V + 0.0372{W_V}^2 \qquad (11)$$

The values of the flow velocity, wind speed, and water depth parameters are given to the model as a time series of measurements and meteorological information [25-26].

- **Nitrification**

Nitrification is another process that affects oxygen balances in the wetland regarding the fact that in the nitrification process, oxygen is consumed when ammonia is converted to nitrite.

$$d(nitrification)/dt = K_4.NH_3.{\theta_4}^{(T-20)}.\frac{DO}{DO + HS\_nitr} \qquad (12)$$

In this equation, K_4 is the rate of nitrification at 20° C (1/day), θ_4 is the temperature coefficient for nitrification, T temperature (°C) and HS_nitr are the semi-saturated concentration for nitrification (mg O_2/l) [25]. The water temperature in the wetland is given to the model in a time series. Based on the previous studies and research, the value of K_4 is between 0.1 to 0.5, the value of θ_4 is considered to be 1.08 [26], and HS_nitr is also suggested to be less than 2 [28].

- **Photosynthesis**

Oxygen production by photosynthesis is associated with the highest production at noon and varies with the time and the length of the day.

$$d(\text{photosynthesis})/dt = \begin{cases} P_{max}.F_1(H).\cos 2\pi\left(\frac{\tau}{\alpha}\right).{\theta_1}^{(T-20)} & if\ \tau \in [t_{up}, t_{down}] \\ 0 & if\ \tau \notin [t_{up}, t_{down}] \end{cases} \qquad (13)$$

This amount of photosynthesis shows the actual production of oxygen in a day (g O_2/m^2/ day). In this equation, P_{max} represents the maximum production at noon (g O_2/m^2/ day), θ_1, the coefficient of temperature for respiration/production in the process of photosynthesis, τ, the real-time of noon, α, the actual length of day, t_{up}, t_{down}, the length, and sunset. $F_1(H)$ is a light adjustment function obtained from the following equation:

$$F_1(H) = e^{-k.H} \qquad (14)$$

In this function, k is the light decay coefficient (m^{-1}), H is the water depth (m), τ, α, t_{up}, t_{down} are parameters that are entered into the model based on time and date as a time series [25]. According to previous studies, in most cases, θ_1 is considered equal to 1.4-2 [29]. Also, the P_{max} value can vary between 3-100 g O_2/m^2/day. Also, the value of k has been suggested between 0.44-0.99, which is considered to be about 0.68 in similar studies [30].

- **Respiration**

Autotrophs and heterotrophs' respiration use oxygen and is described as temperature-dependent.

$$d(\text{respiration})/dt = R_1.F_1(H).{\theta_1}^{(T-20)}) + R_2.{\theta_2}^{(T-20)} \qquad (15)$$

R_1 and R_2 are photosynthetic respiration rates (autotrophs) and animal and bacterial respiration rates (heterotrophs) at 20 °C (g O_2/m^2/day), respectively. θ_2 is the coefficient of temperature for heterotrophic respiration. Respiration determines the actual rate of respiration by plants, bacteria, and animals (g O_2/m^2/day) [25]. According to previous studies, R_1 and R_2 are in the range of 14-24 and 0.036-0.057 $\frac{\mu mol}{m^2}/s$, respectively [31].

- **Sediment oxygen demand**

Sediment oxygen demand due to organic matter that does not come from pollution degradation is described separately. Sediment oxygen demand (SOD) depends on oxygen concentration and temperature as follows:

$$d(sed\ oxygen\ demand)/dt = {\theta_3}^{(T-20)}.\frac{DO}{HS\_SOD + DO} \qquad (16)$$

HS_SOD is the half-saturation concentration for sediment oxygen demand [25]. In this study, sediment modeling has been neglected.

2.2.2 Fecal and total coliform

The majority of commonly occurring waterborne pathogens are linked to human or animal feces. Coliform bacteria are organisms found in the feces of humans and other warm-blooded animals. These bacteria are unlikely to cause disease. Their existence in water resources shows that pathogenic organisms may be present in the environment. Three different groups of coliform bacteria are 1) total coliform, 2) fecal coliform, and 3) Escherichia coli (E.coli). The total coliform group includes an extensive collection of different types of bacteria. Fecal coliforms are part of the total coliform found mostly in human and animal feces, and E.coli is a subsection of fecal coliforms. Typically, there are hundreds to millions of

coliform bacteria per cubic centimeter of untreated wastewater, so the amount of coliform is introduced in terms of number per 100 milliliters.
This model has been developed to track the decay and dispersion of total and fecal coliforms. Bacterial death can be defined as follows:

$$\frac{dC_F}{dt} = -K_{dF}.C_F \qquad (17)$$

where C_F is the concentration of fecal coliforms (1/100 ml) and K_{dF} is the fecal coliforms decay coefficient (1/day). Also, C_F and K_{dF} can be replaced with C_T and K_{dT} to calculate the total coliform decay [25]. According to previous studies, coliform decay coefficient is in the range of 0.26-1 [16].

2.2.3. BOD

The amount of oxygen consumed by microorganisms for degradable materials oxidation within five days is called the 5-day biological oxygen demand or BOD5. Biological oxygen demand is an important indicator for measuring the level of water pollution. Water pollution is the introduction of foreign substances to a body of water which changes the physical, chemical, and biological properties of the water in a suspended or dissolved form. Obviously, the higher number of foreign substances will lead to higher pollution in the water. Measuring the amount of foreign matter through the BOD index is key to determining water pollution level. So, its reduction is considered as an indicator of the wetland's ability for natural purification [32].
Biological oxygen demand is generally divided into three parts: soluble, suspended, and precipitated, each of which can be calculated separately, so one or more equations can define the relation between BOD changes over time. In this study, due to the difficulties in measuring each part separately, the total BOD as the aggregation of three BODs in one equation, has been used in the formulations [25]. Thus, by combining the three parts of BOD in one equation, the rate of BOD changes can be written as follows:

$$\frac{dBOD}{dt} = -BOD_{decay} \qquad (18)$$

The BOD_{decay} itself is defined using the following equation:

$$BOD_{\text{decay}} = K_3.BOD.\theta_3^{(T-20)}.\frac{DO}{DO + HS\_BOD} \qquad (19)$$

BOD is the actual biological oxygen concentration in mgO_2/l, K_3 is the organic matter reduction coefficient at 20°C (1/day), θ_3 is the Arrhenius temperature coefficient, DO is the actual oxygen concentration in mgO_2/l and HS_BOD is the semi-saturated oxygen concentration for BOD ($mg\ O_2/\ l$) [25-26]. In general, the rate of BOD degradation increases with increasing access to oxygen. However, due to the oxygen saturation factor, this increase can be grown to a certain amount of dissolved oxygen concentration as oxygen is soluble in water to a certain extent. The oxygen saturation coefficient, as an experimental value, enters into the equation in the form of a semi-saturated concentration constant at the rate of BOD degradation and varies from system to system. The oxygen saturation coefficient in water depends on salinity, temperature, and air pressure (due to differences in altitude). Dissolved oxygen generally decreases when salinity and temperature increase [33, 34]. According to Chapra [26], K3 and θ3 are in the range of 0.05-0.5 and 1.02-1.09. Also, HS_BOD is proposed equal to 0.128 in similar studies.

2.2.4. Nutrients

2.2.4.1 Nitrogen

The presence of nitrogenous compounds in the sewage can have several adverse impacts on the quality of the receiving waters. Nitrogenous pollution includes compounds with positive and negative charges, including ammonium ions, nitrite, and nitrate. Some adverse effects are [32]:

- The reduction of dissolved oxygen in the receiving waters,
- Toxicity to aquatic life,
- The eutrophication (overgrowth of algae and aquatic plants), and
- Health problems and diseases.

Nitrogen has a complex biological-chemical cycle with multiple biotic/abiotic states, including seven capacities of +5 to -3. These compounds include a variety of inorganic and organic forms of nitrogen that are essential for biological life. The most important mineral form of nitrogen is ammonium (NH_4^+), nitrite (NO_2^-), and nitrate (NO_3^-). Gaseous nitrogen may be present in the form of dinitrogen (N_2), nitrogen oxide (N_2O), nitric oxide (NO_2 and N_2O_4), and ammonia (NH_3) [12].
The change in the main nitrogen states in the wetlands is given in Table 1. Different forms of nitrogen are constantly involved in the chemical conversion of inorganic to organic compounds and the return from organic to inorganic. These processes require energy and are typically derived from an organic carbon source. Other processes release energy, which is used by organisms for growth and survival [12].

Table 1 The transformation of nitrogen in wetlands

Transformation	Process
ammonia-N (aq)→ammonia-N (g)	Volatilization
organic-N→ammonia-N	Ammonification
Nitrification ammonia-	Nitrification

N→ nitrite-N→ nitrate-N	
nitrate-N→ammonia-N	Nitrate-ammonification
nitrate-N→nitrite-N→ gaseous N2, N2O	Denitrification
gaseous N2→ ammonia-N (organic-N)	N2 Fixation
ammonia-, nitrite-, nitrate-N→ organic-N	Plant/microbial uptake (assimilation)
	Ammonia adsorption
	Organic nitrogen burial
ammonia-N→gaseous N2	ANAMMOX (anaerobic ammonia oxidaton)

- **Ammonium**

The ammonium / ammonia equation is defined as follows:

$$\frac{dNH3}{dt} = +ammonium\ yield\ from\ BOD\ decay - transfromation\ of\ ammonium\ to\ nitrate - ammonium\ uptake\ by\ plants - ammonium\ uptake\ by\ bacteria + heterotroph\ respiration \quad (20)$$

This equation includes BOD degradation, nitrification, plant and bacterial consumption, and heterotrophic respiration.

1- Ammonium resulting from BOD degradation is obtained from the following equation:

$$\frac{d(ammonium\ yield\ from\ BOD\ decay)}{\mathrm{dt}} = Y_{BOD}.K_3.BOD.\theta_3^{(T-20)}.\frac{DO}{DO+HS_{DO}} \quad (21)$$

Y_{BOD} is the amount of nitrogen in organic matter in mg NH_3-N/mg BOD. This constant is obtained, based on ammonia nitrogen available. In this study, in spring and summer, Y_{BOD} assumed equal to 0.1018 and 0.1008, based on the ammonia and input BOD [25].

1- The conversion of ammonium to nitrate is expressed as follows:

$$\frac{d(transfromation\ of\ ammonium\ to\ nitrate)}{\mathrm{dt}} = K_4.NH_3.\theta_4^{(T-20)} \quad (22)$$

2- Ammonium consumption by plants

According to the level of complexity that was initially considered, the plant consumption is expressed as follows:

$$\frac{d(ammonium\ uptake\ by\ plants)}{dt} = UN_p.(P - R_1.\theta_1^{(T-20)}) \quad (23)$$

UN_p is the rate of ammonia uptake by the plant (mg N/mg DO)

3-The amount of ammonium absorbed by the bacteria is as follows:

$$\frac{d(\text{ammonium uptake by bacteria})}{dt} = UN_b.K_3.BOD.\theta^{(T-20)}.\frac{NH_3}{NH_3+HS_{NH_3}} \quad (24)$$

UN_b is the rate of ammonia uptake by bacteria (mg N / mg DO) and HS-NH_3 is the semi-saturated concentration for nitrogen uptake by bacteria (mg N/l).

4- Heterotrophic respiration is obtained from the Equation below [25]:

$$\frac{d(heterotroph\ respiration)}{dt} = UN_P.R_2.\theta^{(T-20)} \quad (25)$$

- **Nitrite**

The reactions that affect the mass balance of nitrite are as follows:

$$\frac{dNO_3}{dt} = +\text{transformation of ammonia to nitrite} - \text{transformation of nitrite to nitrate} \quad (26)$$

Equation (26) consists of two terms: ammonia to nitrite conversion and nitrite to nitrate conversion, which are obtained from equations (27) and (28), respectively:

$$\frac{d(\text{transformation of ammonia to nitrite})}{dt} = K_4.NH_3.\theta_4^{(T-20)} \quad (27)$$

$$\frac{d(\text{transformation of nitrite to nitrat})}{dt} = K_5.NO_2.\theta_5^{(T-20)} \quad (28)$$

K_5 is the specific rate of conversion of nitrite to nitrate at 20 °C and θ_5 are the coefficient of conversion of nitrite to nitrate [25]. K_5 and θ_5 for the same conditions are considered equal to 0.5 and 1, respectively [35].

- **Nitrate**

The reactions that affect the nitrate mass equation are as follows:

$$\frac{dNO_3}{dt} = +\text{transformation of nitrite to nitrate} - \text{denitrification} \quad (29)$$

The conversion of nitrite to nitrate is determined from Equation (28) and denitrification is determined from the following equation:

$$\frac{d(\text{denitrification})}{dt} = K_6.NO_3.\theta_6^{(T-20)} \quad (30)$$

K_6 is denitrification rate (1/day) and θ_6 are Arrhenius temperature coefficient (DHI 2014). According to previous studies, $K_6$and θ_6 are in the range of 0.003-1.02 and 1.16, respectively [36].

2.2.4.2 Phosphorus

Phosphorus is a nutrient required by all organisms for the basic processes of life. Phosphorus exists in water in either a particulate phase or a dissolved phase. Particulate matter includes living and dead materials. The dissolved phase also includes inorganic phosphorus and organic phosphorus. Phosphorus in aquatic ecosystems is usually found in the form of phosphates (PO_4^{-3}). Phosphates can be in inorganic form such as orthophosphates and polyphosphates, or organic form such as organically-bound phosphates.

Free orthophosphate is the only inorganic phosphorus that can be used directly by algae and macrophytes. Therefore, it makes a significant link between the two cycles of organic and inorganic phosphorus in wetlands. Another group of inorganic phosphorus compounds is dense linear and cyclic polyphosphates. Organic phosphorus is also found, in phospholipids, nucleic acids, nucleoproteins, phosphorylated sugars, or dense organic phosphates [37].

BOD contains phosphorus, and it is released in the form of orthophosphate when BOD is degraded. According to orthophosphate uptake in algal growth, the equation is interpreted as a function of orthophosphate concentration as below:

$$\frac{dPO_4}{dt} = +phosphorus\ yield\ from\ BOD\ decay - phosphorus\ uptake\ by\ plants - phosphorus\ uptake\ by\ bacteria - heterotrophic\ respiration \quad (31)$$

Equation (31) includes phosphorus from BOD degradation, phosphorus absorbed by plants, phosphorus absorbed by bacteria, and heterotrophic respiration, as the equations (32), (33), (34), and (35):

$$\frac{d(phosphorus\ yield\ from\ BOD\ decay)}{dt} = K_3.BOD.Y_1.\theta_3^{(T-20)}.\frac{PO_4}{PO_4 + HS\_PO_4} \quad (32)$$

$$\frac{d(phosphorus\ uptake\ by\ plants)}{dt} = UP_p.(P - R_1.\theta_1^{(T-20)}) \quad (33)$$

$$\frac{d(phosphorus\ uptake\ by\ bacteria)}{dt} = UP_b.K_3.BOD.\theta^{(T-20)}.\frac{PO_4}{PO_4 + HS\_PO_4} \quad (34)$$

$$\frac{d(heterotrophic\ respiration)}{dt} = UP_P.R_2.\theta^{(T-20)} \quad (35)$$

In these equations, Up_p is the rate of phosphorus uptake by plants and UP_b is the rate of phosphorus uptake by bacteria. HS_PO_4 indicates the semi-saturated concentration of phosphorus absorbed by bacteria [25]. Based on previous studies HS_PO_4 is a function of temperature and phosphate content. For the wetlands, a value equal to 0.065 has been proposed [30].

As mentioned, a customized ecological model has been used to simulate a range of important ecological processes on pollution removal in wetlands. The process formulations consisted of mathematical relations, built-in functions, numbers, constants, and state variables. The arguments were separated by operators and the syntax used for other expressions. The ECO Lab predefined functions like mathematical and built-in functions have been used by referring to them while the other process descriptions were formulated by the user. Hence, the developed model was used to act as a post-processor to calculate the removal dynamics while other models were used to calculate flow and transport processes at each time step. To evaluate the capabilities of the model, the simulation model has been developed for an urban wetland and calibrated based on the field observations.

3. Study area

Gole-Niloufar wetland is an artificial wetland located in the city of Babol, Mazandaran Province, north of Iran. The wetland is placed in the legal territory of the town, surrounded by residential areas and agricultural and barren lands. The wetland's total area is about 38 hectares of common property. The farmers use the outflows for their rice farms. The average depth of the wetland is approximately 2.5 meters. It was constructed and exploited long ago (the exact time is unclear to the authors) by getting water from the Babolroud River through a handmade creek (Aqaroud). The Gole-Niloufar wetland is an Abbandan as defined by Ramsar convection and is constructed by excavation and borders of soil dykes around it (ramsar.org). The Abbandon is a shallow artificial pond in the lowlands south of the Caspian Sea, and its development goes back to hundreds of years. It was used to supply water for rice farming while no pump was available and constant irrigation was needed during the summer growing season. Besides water supply reservoirs in the very flat plains

of the region, Abbandans were always a reliable source of protein for local farmers. Therefore, Abbandans used to play a crucial role in supporting biodiversity and the restoration of the local ecosystem. Although part of these wetlands has been destroyed or degraded, many are still operational, mainly on the city's outskirts. The Gole-Niloufar wetland is probably between a few of those that were left inside the cities, intact and healthful. In the beginning, farmers only used this wetland to irrigate rice and to farm fish. However, since 2017, with the partnership of Babol municipality, it has been restored and allocated as an urban recreation center. The location of the Gole-Niloufar wetland and its inlet creek and outlets are shown in Figure 2.

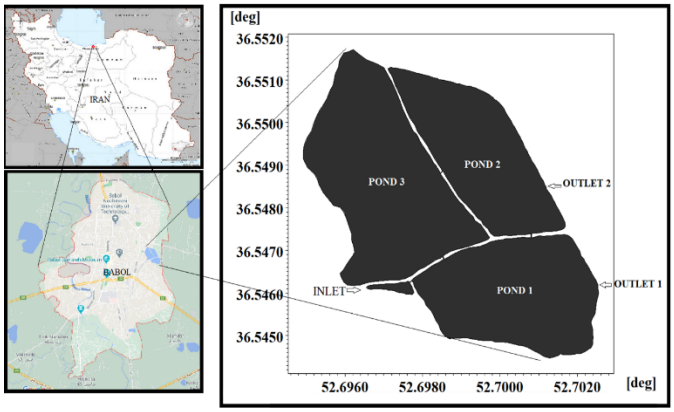

Figure 2. The location of the Gole-Niloufar wetland in the north of Iran and its inlet and outlets

This wetland is composed of 3 ponds that are connected from the below. The wetland's surface is covered with Lotus during the growing seasons, and Phragmites australis also grows in the ponds, which are periodically trimmed. The wetland has one inlet from Aqaroud creek and some outlet pipes; two are opened during growing seasons to discharge water into downstream farms (Figure 2). The diameter of the outlets and ponds connecting pipes is 50 centimeters. A spillway and floodgate control the flow rate at the wetland entrance point. The water's inflow in different seasons –except for special flood events or outflow from upstream- is not much variable due to the flow control for recent recreation purposes. Approximately the same inflow is discharged from the wetland to irrigate the surrounding lands in spring and summer.

The wetland is located in a densely populated area with high human activities and receives domestic sewage from the upstream. A settling pond has been installed at the entrance of the wetland to filter out heavy suspended solids and floating garbage. Due to the wetland's long retention time (about 20-60 days), the incoming contamination is partially treated, especially in the growing seasons. So, the wetland showed a high ability to purify the incoming pollution from Aqaroud Creek. As a result, the turbid and gray water of the inlet becomes clear while leaving the wetland. Due to the presence of Lotus and Phragmites australis, carbon is highly stabilized and fixed in the wetland. The floating plants also uptake nutrients (phosphate and nitrate).

In enclosed and shallow water bodies like wetlands, wind is a crucial factor to create flow at the water surface and depth. Wind-driven circulation is often sufficient to keep the water column well-mixed. Wind data with appropriate temporal and spatial resolution together with the air temperature, evaporation, and precipitation data were obtained from nearby synoptic station (Qarakhil station). The station is located 12 km from the wetland and is the closest synoptic station.

Wetland bathymetry, inflow rate, and velocities at the inlet and outlet were collected from the field measurements. Figure 3 shows the bathymetric map and computational grids for this wetland.

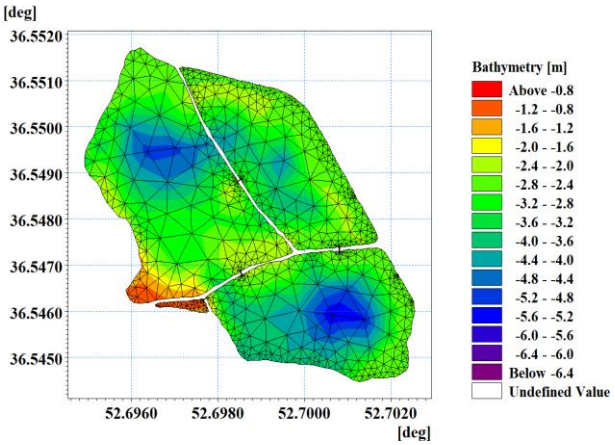

Figure 3. Bathymetric map and computational grids of the Gole-Niloufar wetland

3.1. Calibration process

Hydrodynamic model

More over to bathymetry and computational domain, the hydrodynamic module requires meteorological data and initial and boundary conditions for water level, discharges, and velocities. Infiltration condition, solar irradiance and sink and sources are other important features that need to be defined for the model. Due to the heavy clay soil of the wetland floor, the infiltration was ignored. Figure 4 shows wind speed and direction for Qarakhil station in the summer months i.e. June, July, and August. External forces like the wind will change the hydrodynamic structure of the wetlands. Based on the existing conditions (soil type) and suggested range, bed roughness (K_{dF}) is assumed to be 0.05 in the hydrodynamic model [25].

The effect of wind on surface currents for three periods of high wind was investigated for the performance evaluation of the hydrodynamic model. Wind direction and speed were compared to the resulting velocity in the ponds. Figure 5 shows that the model was properly able to simulate the effects of wind on the surface current. For example, in Figure 5a for the wind maximum speed, 7 m/s, flow also reaches

its maximum (0.225 m/s) at the wetland's surface. The closed boundaries in the wetland lead to the formation of a current on the deeper parts. Therefore, boundaries force surface currents to move downwards and generate weaker currents in the opposite direction. In closed lakes and water bodies, wind is not the only force that produces currents. The other forces are momentum due to flow inlet and changes in temperature and density. These forces, however, were found to be uninfluential due to the low flow rates at the inlet and the wetland's freshwater and non-freezing conditions.

For the flow model validation, floating objects were released at the pond's surface on different occasions, and their movement was tracked visually for some hours before any modeling started for that period. Good agreements were observed later comparing field observations and the results of hydrodynamic simulations. The sensitivity analysis also indicated that the model is sensitive to wind speed and direction changes, and these parameters are the most effective in flow hydrodynamics in the wetland.

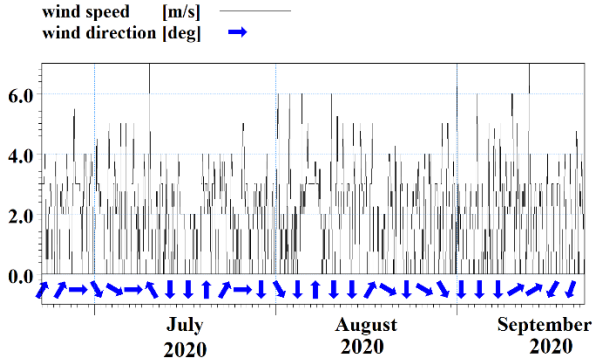

Figure 4. Changes in wind speed and direction during the 2020 summer months, Qarakhil Station

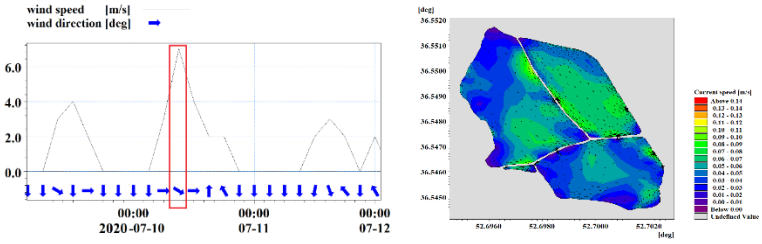

a) Time step 139: 9/7/2020 at 9 o'clock

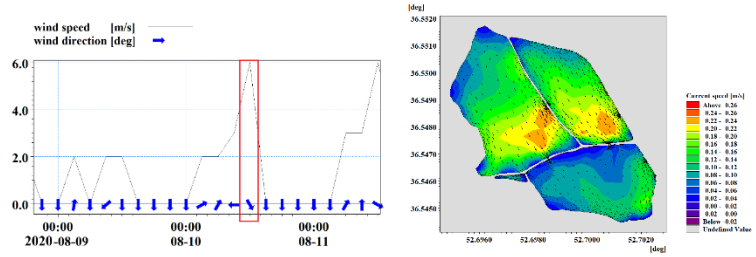

b) Time step 396: 10/8/2020 at 12 o'clock

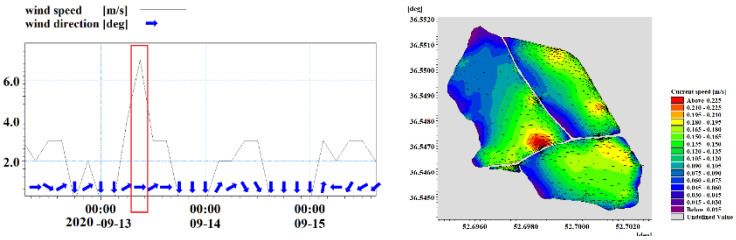

c) Time step 667: 19/9/2020 at 9 o'clock

Figure 5. Wind speed and the resulting surface current in three periods of high wind in the wetland-Pond1

Ecological model

To calibrate the ecological model, BOD_5 concentration was measured at the inlet and outlet of pond 1 at every other day for one month during the summer of 2020 (Table 2). Regarding no changes in water level, the wetland hydrodynamic condition assumed steady state, and the ecological model was calibrated for the natural conditions of Pond 1. Wetland field conditions on Day 1 were set as the model's initial conditions. The coefficients used in the kinetic of each pollutant are critical factors for ecological modeling. Performing different coefficients for the degradation in the proposed ranges, eventually K3, θ3, and HS_BOD were determined equal to 0.2, 1.02, and 0.128 to reach the closest to field observation in the process of BOD_5 calibration. Up to 90% similarity was observed between the results and field measurements using the aforementioned coefficients.

In the sampling month, BOD_5 concentration at outlet 1 changed between 8.09 to 11.12 mg/l. The numerical model calculated BOD_5 concentration at the end of summer equal to 11.45 mg/l in outlet 1 (Figure 6) while the observed value in the field was 11.12 mg/l. Thus, the model prediction was quite close when validated with the field data (Figure 6). To make a long story short, the kinetic of Coliform, Nitrate, and Phosphate in the model was calibrated using the same procedure with the lower sampling frequency. The final coefficients that were employed in the equations above are listed in Table 3.

Table 2. The observed values for BOD_5 in outlet 1 during one-month sampling in summer 2020 (mg/l)

Days	Q (m^3/s)	BOD_5 at inlet	BOD_5 at outlet
day 1	0.025	12.078	8.091
day 3	0.0225	13.188	9.03
day 5	0.0246	13.884	8.94
day 7	0.024	13.545	9.53
day 9	0.031	11.78	8.807
day 11	0.0223	13.476	9.622
day 13	0.022	13.242	9.93
day 15	0.022	12.99	10.024
day 17	0.022	13.2	10.41
day 19	0.023	13.386	10.12
day 21	0.026	14.04	10.513

day 23	0.0244	13.9	10.52
day 25	0.0242	13.85	10.89
day 27	0.0235	13.71	10.85
day 29	0.0221	13.44	11.12

Table 3. The proposed coefficient for the equations of processes

Coefficient	Magnitude	Coefficient	Magnitude
k	0.68	K_{df}	0.4
θ_1	1.6	K_{dt}	0.5
K_3	0.2	R_1	20
θ_3	1.02	R_2	0.152
K_4	0.5	HS_BOD	0.128
θ_4	1.088	HS_nitr	1.9
K_5	0.5	HS_SOD	0.7
θ_5	0.5	HS_PO_4	0.065
K_6	0.5	Y_1	1.5
θ_6	1.16	Y_2	1.2
P_{max}	Spring= 50 Summer= 100	Y_{BOD}	Spring= 0.1018 Summer= 0.1008

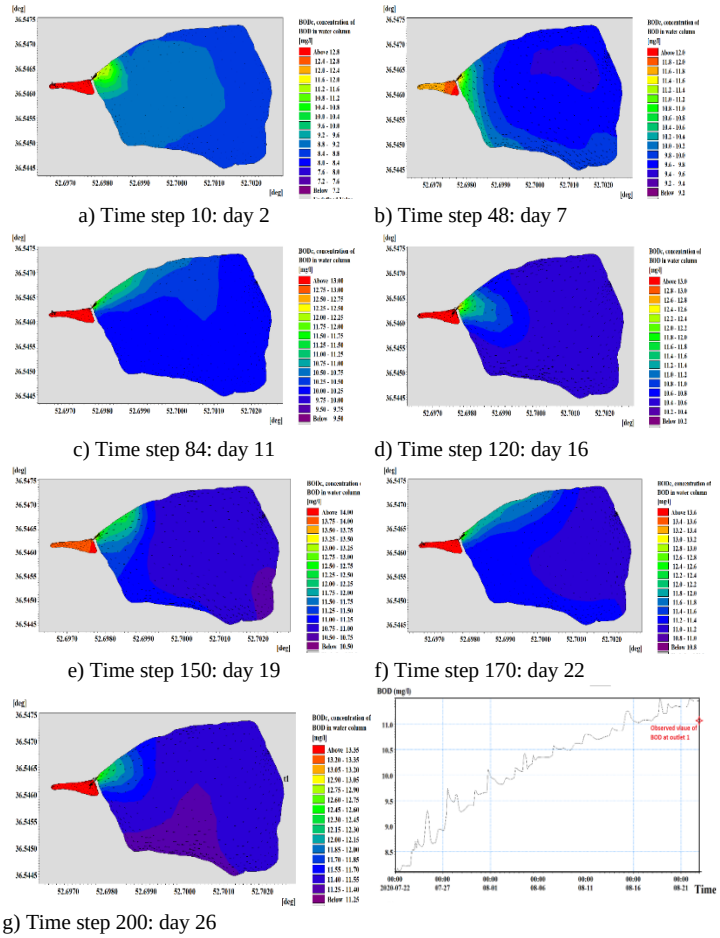

a) Time step 10: day 2 b) Time step 48: day 7

c) Time step 84: day 11 d) Time step 120: day 16

e) Time step 150: day 19 f) Time step 170: day 22

g) Time step 200: day 26

Figure 6. BOD's distribution at the wetland's surface and BOD_5 changes at outlet 1 for the sampling month in summer 2020

4. Results

Following the calibration process, the ecological model was run for two scenarios i.e. only the summer season, and next, spring and summer together. These periods were identified wetland growing seasons with the maximum dynamics. For each series of simulations, field observations were made to find the required data, including the inflow rate, discharge values, and velocities. Wetland inflow was measured equal to 0.153, 0.157, 0.273, and 0.217 m^3/s for spring, summer, fall, and winter. Based on the observation made, the water level was found not to change significantly (almost constant) during the spring and summer seasons. The coliform count, BOD, and nutrient concentrations at the inflow and outlets were measured by sampling in different seasons of 2021. For this purpose, a black bottle of 300 ml was used to collect the water sample. The bottles were sealed and sent to a local laboratory for analysis on the same day. Using the standard methods (Rice et al. 2012), BOD meter, MPN technique, and spectrophotometry the concentration of BOD, coliform, nitrate, and phosphate in the sampling water were determined. The obtained results are shown in Table 4. Also, for the numerical simulations, time intervals equal to 3 hours and 735 timesteps, equivalent to one season, were set for each run.

For the first scenario, the initial condition for concentration was set equal to the field observation at the beginning of summer while in the second scenario, two consecutive seasons, i.e., spring and summer, were simulated with the data of the field that has been modified during the run. In the second scenario, the model has warmed up in the spring season and the data at the end of spring were used as the initial conditions of summer. For verification, results were compared to the field data at the beginning of summer and fall. In the case of only summer simulation, the results were lower than field measured concentration while they were closer to the field data in the second scenario. Therefore, simulations for two consecutive seasons i.e. spring and summer were selected as the case with better accuracy. Figure 7 shows the distribution of BOD_5 concentration at the surface of the wetland for this scenario in summer 2021. As exhibited in the figures, BOD_5 decreases in the wetland while water moves away from the inlet point. In outlets 1 and 2, BOD_5 gradually increases up to reaching maxima at the end of summer. According to our numerical results, shown in Figure 8.a, BOD_5 concentration reached 9.1 mg/l at outlet 1 and 6.9 mg/l at outlet 2 at the end of summer while in the field BOD_5 measured equal to 5 and 3.5 mg/l at this time (beginning of fall season).

Table 4. Total Coliform number, BOD, COD and Nutrition concentration at sampling points in Gole-Niloufar wetland

Fecal coliform			Total coliform		
Inlet	Outlet 1	Outlet 2	Inlet	Outlet 1	Outlet 2

-			25	38	35	Spring
more than 1600	-	-	more than 1600	-	-	Summer
less than 30	less than 30	less than 30	less than 30	less than 30	less than 30	Fall
23	15	7	43	30	15	Winter
COD (mg/l)			BOD (mg/l)			
10	25	25	5.5	14	14	Spring
18	9	9	10	4.9	4	Summer
23	9	6	11	5	3.5	Fall
65	60	55	31	28	26	Winter
Phosphate, PO_4, (mg/l)			Nitrate, NO_3 (mg/l)			
290.14	-		23.66	-		Spring
20	247.37	185.92	4.8	17.94	21.46	Summer
17	38.7	26.9	4	3.5	2	Fall
-	-	-	-	-	-	Winter

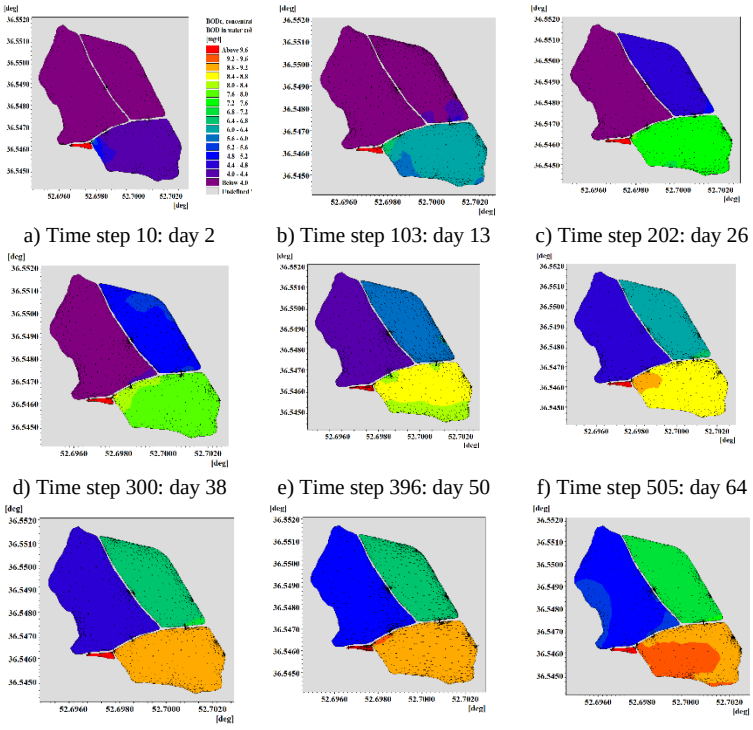

a) Time step 10: day 2 b) Time step 103: day 13 c) Time step 202: day 26

d) Time step 300: day 38 e) Time step 396: day 50 f) Time step 505: day 64

g) Time step 590: day 74 h) Time step 667: day 84 i) Time step 735: day 93

Figure 7. The distribution of BOD at surface of the Gole-Niloufar wetland in the summer of 2021

Similarly, the model calculated the extent of changes in pollutant concentrations for total coliform, nitrate and phosphate as shown in Figure 8 b, c and d. For the study condition, coliform concentration was more than 1600 MPN/100 at the inlet point. Figure 8.b shows the changes in total coliform at outlets 1 and 2 during the summer of 2021. According to the existing trends, after increases in total coliform at the beginning of summer it reaches 1402 MPN/100ml at outlet 1 and 869 MPN/100ml at outlet 2 at the end of summer. So the results show a slight reduction in total coliform while the contaminated water flows through the wetland. During the springtime, the load of coliform was low but in summer it grew from 13.75 to 1400 MPN/100ml in outlet 1 and from 21.7 to 870 MPN/100ml in outlet 2.

Figure 8. c shows the dynamic of nitrate removal in outlets 1 and 2. According to these curves, at the end of summer nitrate reaches 6.18 mg/l in outlet 1 and 9.92 mg/l in outlet 2. During the summer, the factors that consume nutrients in the wetland are more active and it leads to distinctive decreases in the concentration of nitrate. Transformation of nitrogenous compounds, heterotrophic respiration, and the consumption by plants and bacterial uptake are the main processes of nitrogen consumption in wetlands. Figure 8.d also demonstrates the changes in phosphate concentration in outlets 1 and 2 in the summer of 2021. According to these curves, at the end of summer, phosphate reaches 29.96 mg/l in outlet 1 and about 56.86 mg/l in outlet 2. Because the plants are fully grown in the summer, wetlands could significantly decrease phosphate concentration in this season. Bacterial activity in the wetland is also at its maximum in the summer which leads to a good removal of nutrients in wetlands.

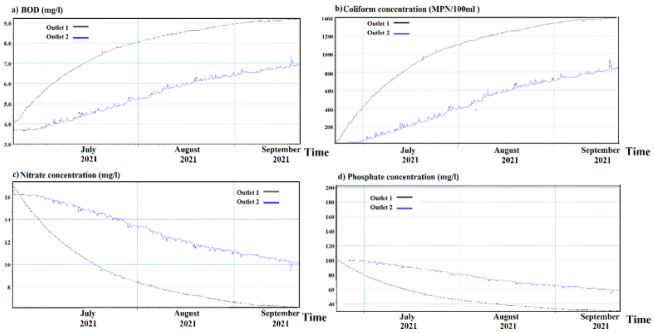

Figure 8. The changes of a) BOD concentration b) total coliform number c) nitrate d) phosphate in Gole-Niloufar wetlands' outlets 1 and 2 in summer 2021

Quality standards

Table 7 shows the water quality standards for different uses based on Iran's environmental regulations [38]. There are Iran's national water quality standards for BOD, COD, and coliform content in agricultural use (raw and non-raw crops), recreation, aquatic life, fish farming, and water supply [39]. Comparing the data obtained from the field sampling and model with the standards, it can be concluded that this wetland was not suitable for cold-water fish farming in spring due to excessive BOD. It, however, was in the range for warm-water fish farming. BOD and COD of water at outlets 1 and 2 were found to be suitable for agricultural purposes. Besides the concentration of organic matter, the microbial load is an important parameter for water's different uses. The amount of fecal and total coliform was relatively low in the spring, so the water can be used for all purposes except drinking. Due to excessive BOD, the water entering the wetland was not suitable for both cold and warm-water fish farming in the summer. Wetland's outflow, however, was suitable for rice

farming in terms of BOD and COD in summer, while was highly contaminated in terms of microbial pollution for direct contact. From the matter of the microbial content, the wetland's water was unsuitable for recreation, in which, people must be prohibited from direct contact (swimming or showering) for whole seasons.

Table 5. Iran's standards for water use in recreation, water supply, and agriculture [38,39]

Fecal coliform	Total coliform		
400	1000	The standard for discharge to surface water	
400	1000	Irrigation standard	
less than 100	-	Crops that consumed raw, sports fields, public parks	Agricultural uses
doesn't have a limit	-	Grains, industrial products, forage, pasture, and trees	
400	2000	Direct	Direct recreational uses
2000	5000	Indirect	
20	50	Water quality standards for drinking water resource	
100	460	Water quality standards for swimming	
COD	**BOD_5**		
60	30	Limitation for discharge to surface water	
200	100	Irrigation	
-	less than 3	group 1*	
-	less than 6	group 2**	
-	less than 3	quality standards for drinking water use	

*Group 1: Ecosystems suitable for cold-water fish
**Group 2: Ecosystems suitable for warm water fish

Discussion

Comparing calculated data from our numerical simulations with the field observations generally showed that the Gole-Niloufar wetland was particularly effective at removing excess nutrients, such as nitrogen and phosphorus, from water while was not that effective on BOD and coliform degradations to the expected extent. Gole-Niloufar wetland acts as a nutrient sink, capturing and retaining nutrients through various processes i.e. plant uptake and microbial processes. However, wetland showed limited capability to break down and remove organic pollutants and mineralize them. Natural treatment and inactivation of pathogens in wetlands depend on vegetation and the physical, chemical, and biological conditions and our findings have shown that the warm climate of summer in the study area will make wetlands to be less effective in that aspect of coliform removal.

Results also show that despite considering various chemical and biological processes, the model was able to only evaluate the generic trends of wetland impact on downstream water quality and could not accurately estimate pollutant concentrations or removal rates. Simulating the fate and transport of pollutants in the wetland is a very complex process and needs very high data resolution of pollutant loadings, environmental conditions, and wetland characteristics. Although the model exhibited good accuracy in the process of calibration when simulated with high-resolution data for one month in pond 1, the results were not same good for the whole season when load changes of contamination during the simulation period were not considered. So, the model was good in ecosystem services modeling to assess the overall benefits provided by wetlands but not reliable for long-term modeling of the complicated conditions of pollutant loadings, complex geometries, and imprecise environmental states. The authors believe that considering other processes that were ignored here like sorption, desorption, sedimentation and precipitation, volatilization, nutrient cycling, and microbial reactions in future studies will help to increase model comprehensiveness and sufficiency.

5. Conclusions

Wetlands and cities have always been in an uneasy relationship and disparate mutual effects. Healthy wetlands are a critical element to sustainable cities, as they can provide a natural defense against extreme floods and can filter water from human-caused activities. In this study, a new template has been developed for the ecological modeling of urban wetlands from the perspective of wetlands' natural ability to retain contaminants and improve water quality. Wetlands are multi-purposed ecosystems that can purify water through flow retention, nutrient uptake, removal of organic matter, microbial degradation, and transformations besides sustaining local biodiversity. In the model, the kinetic of complex biological and chemical transformation of organic pollutants, together with the physical processes of pollutant removal and purification, were disclosed and mathematically simulated. The main objective was to develop a customized template for the modeling of both hydrodynamic and ecological features in urban wetlands. So, a numerical model has developed to solve the equations of state variables for the affecting process. The model has been tested for a wetland in the north of Iran, at the Babol city. The city has several wetlands in its territory and neighborhood and is located only 190 km from the city of Ramsar, where the wetland world-known convention was born. Wetland was first simulated for one month in the summer of 2020, and then the results were compared to the field data for model calibration and validation. To ensure model accuracy, the model was run for 2 seasons, i.e., spring and summer of 2021, each equivalent to 93 days with 735 timesteps. The results showed concentration reduction for BOD, total coliform, phosphate, and nitrate up to 45%, 44.96%, 44.8%, and 43.47%, respectively. The results were found to be reasonably close to the field data. Wetland's ability to improve water quality for the designated applications, i.e., recreation, agriculture, and fish farming was also evaluated by comparing

them to Iran's environmental quality standards for water use. Wetlands water was found to be often suitable for warm-water fish farming and agriculture while it was unappropriated for swimming or recreation purposes.

According to the observations made, it can be concluded that the wetland in its active season (summer) works well in terms of natural treatment and could reduce pollution to a desirable level. This newly developed setup of ECO Lab template can be used for the purification prediction in natural and constructed wetlands while still, degradation kinetics and reaction rate of the pollutants need to be locally investigated.

6. References

[1] World Cities Report. (2020), The value of sustainable urbanization. Nairobi,

[2] Zhongming, Z., Linong, L., Xiaona, Y., Wangqiang, Z. & Wei, L. (2020). World Cities Report 2020: The Value of Sustainable Urbanization.

[3] Mitsch, W.J., Bernal, B. & Hernandez, M.E. (2015) Ecosystem services of wetlands. International Journal of Biodiversity Science, Ecosystem Services & Management, 11(1), pp.1-4.

[4] Finlayson, C., Bartlett, M., Davidson, N. & McInnes, R. (2013). The Ramsar Convention and urban wetlands: an opportunity for wetland education and training. In Workbook for managing urban wetlands in Australia (pp. 34-51). Sydney Olympic Park Authority.

[5] Gardner, R.C. & Davidson, N.C. (2011). The ramsar convention. Wetlands: Integrating multidisciplinary concepts, pp.189-203.

[6] Frazier, S. (1999). Ramsar sites overview. Wetlands International.

[7] Matthews, G.V.T. (1993) March. The Ramsar Convention on Wetlands: its history and development. Gland: Ramsar Convention Bureau.

[8] Bai, J., Cui, B., Cao, H., Li, A., & Zhang, B. (2013) Wetland degradation and ecological restoration. The Scientific World Journal, 2013.

[9] Hammer, D.A. (1989). Constructed Wetlands for Wastewater Treatment: Municipal, Industrial, and Agricultural. Lewis Publishers.

[10] Craft, C. (1997). Dynamics of nitrogen and phosphorus retention during wetland ecosystem succession. Wetlands Ecology and Management 4:177–187.

[11] Mitsch, W.J., & Gosselink, J.G. (2007). Wetlands (4th ed.). Wiley.

[12] Vymazal, J. (2007) Removal of nutrients in various types of constructed wetlands. Science of the total environment, 380(1-3), pp.48-65.

[13] Vymazal, J. (2013). Plants in constructed, restored and created wetlands. *Ecological engineering*, *61*, pp.501-504.

[14] Somes, N.L., Bishop, W.A., & Wong, T.H. (1999) Numerical simulation of wetland hydrodynamics. Environment International, 25(6-7), pp.773-779.

[15] Kazezyılmaz-Alhan, C.M, Medina, Jr MA., & Richardson, C.J. (2007) A wetland hydrology and water quality model incorporating surface water/groundwater interactions. Water Resources Research, 43(4).

[16] Boutilier, L, Jamieson, R, Gordon, R., & Lake, C. (2011) Modeling E. coli fate and transport in treatment wetlands using the water quality analysis and simulation program. Journal of Environmental Science and Health Part A, 46(7), pp.680-691.

[17] Suntoyo, Ikhwani, H., Zikra, M., Sukmasari, N.A., Angraeni, G., Tanaka, H., Umeda, M., & Kure, S. (2015). Modelling of the COD, TSS, Phosphate and Nitrate Distribution Due to the Sidoardjo Mud Flow into Porong River Esruary. Proccedia Earth and Planetary Science, 14, pp. 144-151.

[18] Qiao, H, Zhang, M, Jiang, H, Xu, T, & Zhang, H. (2018) Numerical study of hydrodynamic and salinity transport processes in the Pink Beach wetlands of the Liao River estuary, China. Ocean Science, 14(3), pp.437-451.

[19] Pugliese, L., Kusk, M., Iversen, B.V. & Kjaergaard, C. (2020). Internal hydraulics and wind effect in a surface flow constructed wetland receiving agricultural drainage water. Ecological Engineering, 144, p.105661.

[20] Thu Minh, HV, Tri, VPD, Ut VN., Avtar, R. Kumar, P., Dang, TTT., & Downes, NK. (2022). A Model-Based Approach for

Improving Surface Water Quality Management in Aquaculture using MIKE 11: A Case of the Long Xuyen Quadangle, Mekong Delta, Vietnam. Water, 14(3), 412.

[21] DHIgroup. (2023). MIKE 21 & MIKE 3 Flow Model FM. MIKE Ecolab module short description, DHIheadquarter, agern alle 5, Dk 2970 Hørsholm Denmark.

[22] DHI. (2014). MIKE 3 FLOW MODEL Hydrodynamic Module Scientific Documentation, DHI Water & Environment, Horsholm.

[23] Ramezani, M., Abessi, O., & Firoozjaee, AR. (2021) Effect of proximity to bed on 30° and 45° inclined dense jets: a numerical study. Environ. Process. 8, 1141–1164.

[24] Ramezani, M., Abessi, O., Firoozjayee, AR. (2020) Numerical simulation of dense discharges from 30° submerged inclined jet in free and bed-affected conditions (in Persian). J. Hydraul. 15, 75–91.

[25] DHI. (2014). ECO LAB 1D, 2D and 3D Water Quality and Ecological Modelling User Guide, DHI Water & Environment, Horsholm.

[26] Chapra, SD. (1997) Surface water quality modeling, 1st Ed., MC Grawhill, New York.

[27] Moran, S. (2018) An Applied Guide to Water and Effluent Treatment Plant Design. Butterworth-Heinemann.

[28] Law, Y, Matysik, A, Chen, X, Thi, SS, Nguyen, TQN, Qiu, GL, Natarajan, G, Williams, RB, Ni BJl Seviour, TWl, & Wuertz, S. (2018) Apparent oxygen half saturation constant for nitrifiers: genus specific, inherent physiological property, or artefact of colony morphology, p.289645.

[29] Larcher, W. (2003) Physiological plant ecology: ecophysiology and stress physiology of functional groups. Springer Science & Business Media.

[30] Williams, AS., Kiniry, JR., Mushet, D., Smith, LM., McMurry, S., Attebury, K., Lang, M., McCarty, GW., Shaffer, JA., Effland, WR., & Johnson, MVV. (2017) Model parameters for representative wetland plant functional groups. Ecosphere, 8(10), p.e01958.

[31] Hew, CS., Krotkov, G., & Canvin, DT. (1969) Determination of the rate of CO2 evolution by green leaves in light. Plant physiology, 44(5), pp.662-670.

[32] APH Association, & Federation, WE. (2005) Standard methods for the examination of water and wastewater. American Public Health Association (APHA): Washington, DC, USA.

[33] Amrizal, M. (200) Effect of Dissolved Oxygen Concentration on BOD Decay. University Technology Petronas.

[34] Banks, CJ., Koloskov, GB., Lock, AC., & Heaven, S. (2003) A computer simulation of the oxygen balance in a cold climate winter storage WSP during the critical spring warm-up period. Water science and technology, 48(2), pp.189-196.

[35] Guo, J., Peng, Y., Huang, H., Wang, S., Ge, S., Zhang, J., & Wang, Z. (2010) Short-and long-term effects of temperature on partial nitrification in a sequencing batch reactor treating domestic wastewater. Journal of Hazardous Materials, 179(1-3), pp.471-479.

[36] Climate Policy Watcher, (2010) The Influence of Dissolved Oxygen on the Nitrification Rate (https://www.climate-policy-watcher.org/nitrogenremoval/the-influence-of-dissolved-oxygen-on-the-nitrification-rate.html

[37] Vymazal, J. (1995) Algae and element cycling in wetlands. Chelsea, Michigan: Lewis Publishers. 698 pp.

[38] Department of Environment. (2016), Standards of water quality of Iran, Deputy of Human Environment, Islamic Republic of Iran

[39] Department of Environment. (2012), Human Environmental Laws, Regulation, Criteria and Standards, Deputy of Human Environment, Islamic Republic of Iran.